Detection of a Fermi-level crossing in Si(557)-Au with inverse photoemission

J. A. Lipton-Duffin, J. M. MacLeod, and A. B. McLean*
Department of Physics, Queen's University, Kingston, Ontario, Canada K7L 3N6
(Received 25 February 2006; revised manuscript received 24 April 2006; published 19 June 2006)

The unoccupied energy bands of the quasi-one-dimensional (1D) Si(557)-Au system have been studied with momentum-resolved inverse photoemission. A band is found that lies (0.4±0.4) eV above the Fermi level at the center of the surface Brillouin zone ($\bar{\Gamma}$). It disperses to higher binding energy, along the $\overline{\Gamma K}$ direction, and crosses the Fermi level at $k_{\|}=0.5\pm0.1$ Å^{-1}. The corresponding direction in real space is parallel to both the rows of silicon adatoms and the rows of embedded gold atoms that are distinctive features of this surface reconstruction. The location of the crossing is in good agreement with previously published photoemission data [Altmann *et al.*, Phys. Rev. B **64**, 035406 (2001); Ahn *et al.*, Phys. Rev. Lett. **91**, 196403 (2003)], where two closely spaced bands were found to disperse from the $\bar{K}$ zone boundary to lower binding energy and then cross the Fermi level. In addition to the band mentioned above, a band was found that has parabolic dispersion along $\overline{\Gamma K}$, the direction that is parallel to the rows of embedded gold atoms. The band minimum for the parabolic band lies (0.8±0.4) eV below the vacuum level and it has an effective mass $m^*=(1.0\pm0.1)m_e$, where m_e is the free electron mass. Perpendicular to the rows of gold atoms, as expected for a state with quasi-1D symmetry, it has flat dispersion. This band may be an image state resonance, overlapping the silicon conduction band continuum, and it is spatially localized to the edge of the silicon terraces.

DOI: 10.1103/PhysRevB.73.245418 PACS number(s): 73.20.At, 73.21.Hb, 79.60.Jv, 68.37.Ef

I. INTRODUCTION

Quasi-one-dimensional (quasi-1D) systems can be grown on surfaces and used to study the electronic and magnetic properties of electrons that are confined to a single spatial dimension.[1–6] Several different growth methodologies have been explored (e.g., Fig. 1). The most straightforward approach is to select overlayer phases that have quasi-1D symmetry such as Cu(100)-Tl (Refs. 7 and 8) or Si(111)-In(4 $\times$1).[9] One of the first studies of a surface quasi-1D system was performed on Cu(100)-Tl, and evidence was found for a one-dimensional electronic structure within the rows of thallium atoms and a Peierls-like energy gap persisting to room temperature.[7,8] However, in the study of metal to nonmetal phase transitions in quasi-1D overlayer phases, semiconductor substrates are frequently used because there are, by definition, no bulk states in the fundamental energy gap.[10] Consequently, overlayer phases can be grown on these substrates and the region around the Fermi level can be studied with spectroscopic techniques, such as photoemission, inverse photoemission, and scanning tunneling spectroscopy (STM), without interference from the bulk bands in the substrate. This greatly simplifies the interpretation of the experimental data and makes the identification of gap openings in the overlayer band structure much more straightforward.

In addition to the quasi-1D overlayer phases mentioned above, that can be grown on nominally flat surfaces, vicinal surfaces can also be used to support a variety of quasi-1D overlayer phases [Figs. 1(b) and 1(c)]. The advantage of using vicinal surfaces is that the spacing between the individual adatom rows or "wires" can be changed by using different offcut angles. Moreover, if one of the "magic" offcut angles is used,[10,11] the atomic steps become a natural part of the surface reconstruction and the dispersion in the terrace width is reduced to the point where it is effectively zero. In particular, techniques have recently been developed for assembling parallel rows of gold atoms on vicinal silicon surfaces.[10–15] For example, the Si(557)-Au system contains one row of gold atoms embedded in each silicon terrace, lying parallel to the steps that terminate the terraces. The gold inter-row spacing is equal to the silicon terrace width of 1.9 nm. At this spacing, the coupling between the rows of gold atoms is weak and the two-dimensional system effec-

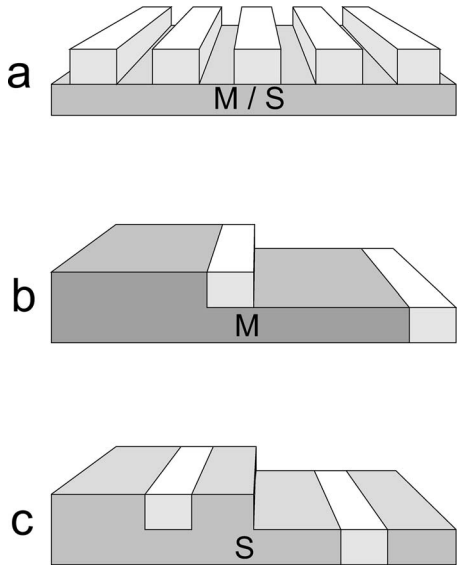

FIG. 1. Schematic representation of three different types of surface quasi-1D systems. (a) A quasi-1D overlayer phase comprising parallel rows of adatoms on a metal (M) or semiconductor (S) substrate. (b) A vicinal metal surface with adatoms decorating the steps to produce a one-dimensional "wire." (c) A vicinal semiconductor surface with atoms embedded in the terraces.

tively becomes a one-dimensional system. However, by using a vicinal surface with a steeper offcut relative to (111), such as (553), the terrace width can be reduced to 1.5 nm and the inter-row coupling can be increased. The increased coupling can be seen in the energy bands near the Fermi level using angle-resolved photoemission.[11] Consequently, the coupling between the adatom rows that comprise the quasi-1D structure can, to some degree, be tailored.

Interestingly, studies of the Si-Au quasi-1D overlayer systems have found multiple energy bands that are fractionally filled, giving rise to nested sheets at the Fermi surface.[11] Some, but not all, of these bands are metallic at room temperature and undergo metal to nonmetal transitions when the system is cooled below room temperature.[11,16,17] It is thought, although the view is not universally held,[18] that the metal to nonmetal transitions in these systems are Peierls instabilities. Moreover, it is expected that electron correlations in these quasi-1D systems with fractionally filled bands will give rise to exotic electronic phases such as the Luttinger liquid.[1–3,10] This is the primary reason why these systems have been the subject of so much attention. In fact, early studies of the Si(557)-Au system suggested evidence for the absence of fermionic quasiparticles and the separation of spin and charge into collective spin and charge fluctuations.[10,19] Although this exciting possibility was later ruled out by a more detailed angle-resolved photoemission study of the energy bands,[14] that exploited the tuneable nature of synchrotron radiation to maximize the photoemission cross section of the two bands, their physical origin has not yet been satisfactorily established. For example, there is still a poor level of agreement between the experimental[10,11,13,14] and *ab initio* theoretical band structures[18,20,21] that may be due, at least in part, to the complexity of the surface reconstruction and the influence of the embedded gold atoms on the electronic structure.

The two occupied bands (S1 and S2) that have been observed just below the Fermi level in the Si(557)-Au system both have a parabolic dispersion and resemble the spin-orbit split surface states that exist in the neck of the bulk Fermi surface near the L point on Au(111).[22] The role of relativistic corrections to the band structure in the Si(557)-Au system has been investigated with *ab initio* theoretical approaches,[18] and it was demonstrated that the spin-orbit interaction does generate two bands that have a similar dispersion over a large part of the surface zone. However, recent temperature dependent experimental studies[16,23] performed with STM and angle-resolved photoemission have shown that S1 and S2 behave quite differently. The S2 band is gapped at room temperature whereas S1 is metallic. Upon cooling, a gap opens in the metallic S1 band. The gapped S2 band has been associated with the silicon adatoms in the $2\times$ row that are rigidly constrained by bonds to the substrate. In contrast, the metallic S1 band has been associated with silicon atoms at the terrace edge that undergo a Peierls-like periodic lattice distortion. In this scenario the electronic phase transition is localized to the terrace edges. It is not clear how this observation can be reconciled with the *ab initio* calculations that attribute the origin of the S1 and S2 bands to the spin splitting of a single band.

Clearly, further work is required to resolve this issue and to provide a consistent description of this complex system.

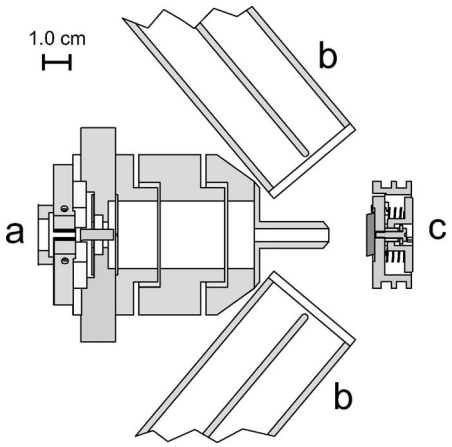

FIG. 2. The electron source (a), the two isochromat photon detectors (b), and the sample/holder (c) used in the inverse photoemission experiment. The photon detectors make an angle of 50° with the high symmetry axis of the source. They are both mounted on linear drives so that they can be pushed past the electron source to increase the solid angle of detection (see the text).

The aim of the present study is to provide a more complete picture of the experimental band structure by measuring the bands that lie above the Fermi level using inverse photoemission.

II. EXPERIMENTAL DETAILS

The inverse photoemission experiments were performed with a homebuilt instrument comprising a Stoffel-Johnson low energy electron source[24] and two ethanol filled Geiger-Müller photon detectors.[25,26] The photon detectors operate in isochromat mode, are run concurrently to maximize photon detection, have a detection energy of $\hbar\omega=(10.78\pm0.01)$ eV, and have a full width at half-maximum bandpass $\Delta\hbar\omega$ of (0.37 ± 0.02) eV. Because the system that we studied in this paper has a low inverse photoemission cross section,[27] it was necessary to use the full collection angle of π steradians offered by our system by pushing the photon detectors close to the sample (Fig. 2). The STM images were acquired at room temperature with a homebuilt beetle-type microscope,[28,29] using a mechanically formed platinum-iridium tip.

Si(557) wafers (Virginia Semiconductor Inc.) were prepared by cutting a single-crystal ingot 9.5° away from the (111) plane towards $[\bar{1}\bar{1}2]$. The wafers were then diced into rectangular samples with a width of 6 mm and a length of 17 mm. After transfer into vacuum, the samples were degassed overnight by resistive heating, using a slow linear ramp from room temperature to 850 °C while keeping the pressure in the vacuum chamber below 2×10^{-9} Torr. The samples were repeatedly flashed to 1250 °C to remove the native oxide, then quickly cooled to 850 °C, and held at this temperature for 10 min to promote the formation of long-range order. They were subsequently cooled at a rate of $\simeq1$ °C/s. The cleaned samples were then transferred into a preparation chamber and 0.2 monolayers (ML) of gold were

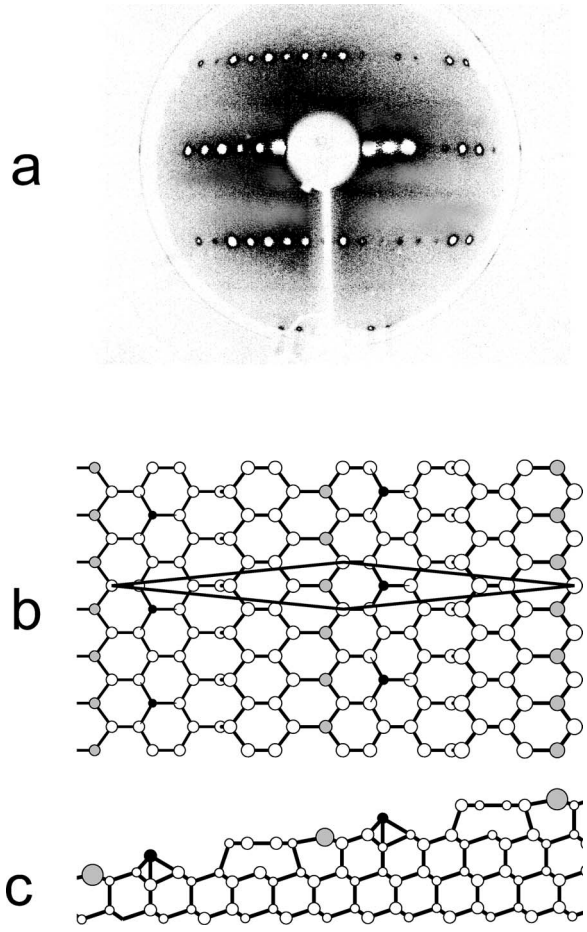

FIG. 3. (a) A low energy electron diffraction image at a primary beam energy of +80 eV. The contrast has been enhanced to emphasize the 2× streaks that appear as horizontal lines between the main diffraction spots. Panels (b) and (c) show the top and side views of a structural model for Si(557)-Au (Ref. 11). The solid lines in panel (b) define the 1×1 unit cell. The full black circles represent silicon adatoms and the full light gray circles are gold atoms.

evaporated from a tungsten basket at a rate of 0.01 Å/s. During the deposition, the temperature was held at 600 °C. Following the deposition, the samples were ordered by a brief flash to 850 °C followed by a cooldown at ≃1 °C/s. This preparation method consistently produced ordered surfaces, as judged by STM, and sharp electron diffraction patterns.

III. RESULTS

Figure 3(a) presents a low energy electron diffraction (LEED) image collected from the Si(557)-Au system. Panels (b) and (c) of the same figure are top and side views of the geometric structure that minimizes the total energy.[11] The structure may be thought of as a series of Si(111) terraces separated by a single-height step that each contain an embedded row of gold atoms. The silicon atoms located near the step edges are π-bonded. Consequently, they have a similar bonding configuration to the silicon atoms in the Si(111)(2 $\times1$) reconstruction,[30] and also the silicon atoms in the honeycomb chain-channel reconstruction for the alkali metal-3 $\times1$ systems.[31] In addition, the translational periodicity of the unit cells is doubled by the presence of the Si adatoms shown in black in Fig. 3(b). Notice that there are faint 2× streaks in the LEED pattern (horizontal lines) that indicate that the rows of silicon adatoms [Fig. 3(b)] are out of registry with one another. This is consistent with our STM images of Si(557)-Au, one of which is reproduced in Fig. 4. The brightest features in this constant-current topograph are thought to be an irregular array of extra silicon adatoms that are displaced during gold adsorption. It is clear that these extra silicon adatoms do not form a 2D translationally periodic superlattice. There are also rows of bright protrusions that have a spacing of (7.6±0.8) Å, twice the 1×1 lattice constant (a_o=3.84 Å), suggesting that they are the silicon adatoms that are shown in black in Figs. 3(b) and 3(c). The other notable feature in this image is the array of streaks that run parallel to the rows of silicon adatoms and have recently been attributed to step edges.[16,23]

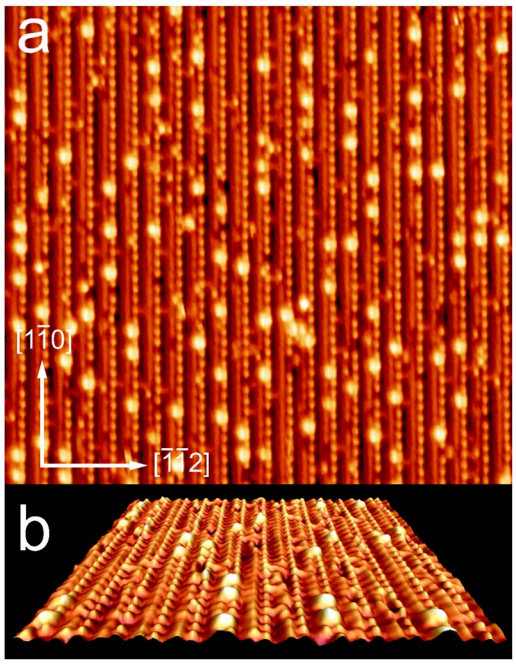

FIG. 4. (Color online) (a) An STM image of the Si(557)-Au system. The image area is 41 nm×41 nm and the sample bias was +1.87 V (unoccupied states). The silicon adatoms that form rows with a 2× periodicity are evident, as are the streaks that are thought to arise from the silicon atoms located at the terrace edge. (b) A higher magnification image of the same surface, taken with a sample bias of +2.00 V, showing the silicon 2×1 adatom rows, the extra silicon adatoms, and the short terraces that are inclined at 9.5°. The image area is 25 nm×25 nm.

Figure 5 is a stack plot of inverse photoemission spectra containing a sequence collected with the electron source in the [$\bar{1}$10] azimuth and displaced from the sample normal by the angle θ, up to a maximum of $\theta=+45°$. This direction is parallel to the rows of atoms [Figs. 3(b) and 3(c)]. The register line[32] lies along the $\overline{\Gamma K}$ direction in reciprocal space, and this is indicated by the dashed line in Fig. 5. Four distinct features, labeled A–D in the figure, are observed. This

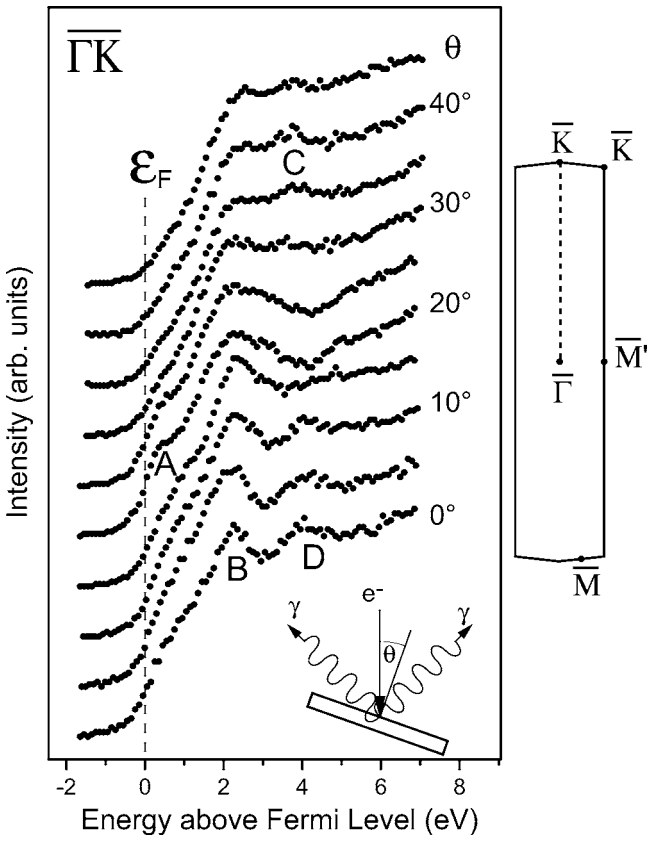

FIG. 5. A stack plot of inverse photoemission spectra generated by rotating the sample relative to the incoming electron beam in 5° increments away from [557] towards [$\bar{1}$10]. The surface Brillouin zone is also shown (right). High symmetry points have been labeled (Ref. 20) and, in the experiment, the $\bar{\Gamma}K$ line (shown dotted) was probed.

data set was also transformed to a $(E,k_{\|})$ grid and differentiated twice to emphasize the portions of the spectra that have high curvature (Figs. 6 and 7). A similar procedure has previously been used to render occupied energy bands using angle-resolved photoemission.[33]

A control experiment was performed on the clean Si(557) surface to help identify the features that are produced by the reconstruction of the surface and the addition of gold adatoms. The data from Si(557) are plotted to the left of the $\bar{\Gamma}$ line in Fig. 6. The data on both the left- and the right-hand side of the $\bar{\Gamma}$ were collected using the same experimental geometry; they have simply been mirror reflected about $\bar{\Gamma}=0$ so that they can be combined in the same panel plot. A number of subtle changes in the band structure of the Si(557) surface are observed when gold adatoms are added and the surface reconstructs. When gold adatoms are added to the surface, weight is transferred from the feature labeled A to the feature labeled B (see later). Moreover, the latter shows very little dispersion with $k_{\|}$. The feature behaves similarly on the clean surface, though it does not dominate the spectrum to the same extent.

At $k_{\|}\approx 0.5$ Å^{-1} (Fig. 6), or alternatively $\theta\approx 20°$ (Fig. 5), it is clear that feature A does not lose intensity as it approaches the Fermi level, suggesting that a band, or a

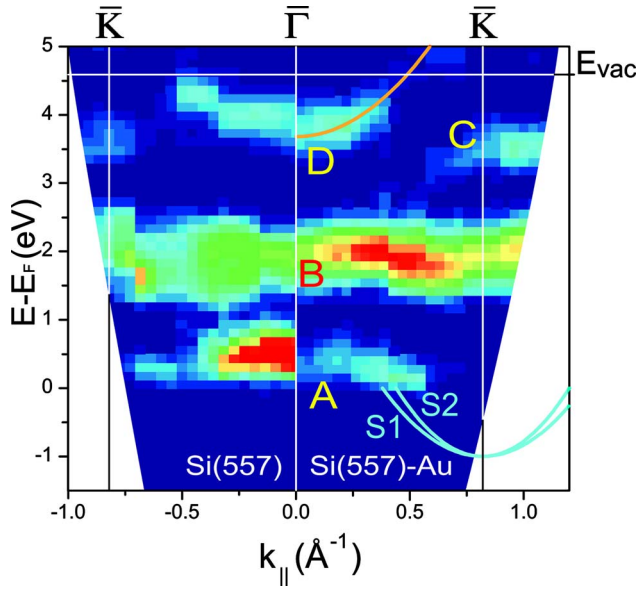

FIG. 6. (Color online) The data from Fig. 5 mapped to a $(E,k_{\|})$ grid. The $(E,k_{\|})$ mapping for Si(557)-Au is shown to the right of the $\bar{\Gamma}$ line, and the corresponding data from clean Si(557) are on the left. The bands labeled S1 and S2 (turquoise) are described in the text and E_{vac} denoted the position of the vacuum level. Curve D (orange) is a free-electron-like parabola with an effective mass of $m^{*}=(1.0\pm0.1)m_e$ fitted to feature D in the Si(557)-Au data.

closely spaced doublet, crosses the Fermi level at $k_{\|}=(0.5\pm0.1)$ Å^{-1}, in agreement with previous photoemission studies.[13,16] The earlier of these two studies[13] found two closely spaced bands, labeled S1 and S2 in Fig. 6, which crossed the Fermi level at $k_{\|}=0.38$ and 0.44 Å^{-1}, respectively. This corresponds to incidence angles of 17.6° and 20.6° in our experiment. The later study[16] found the Fermi level crossing to occur at $k_{\|}=0.35$ and 0.41 Å^{-1}, respectively.

The two bands have a splitting of only 0.3 to 0.4 eV.[16] Consequently, the individual bands cannot be resolved with

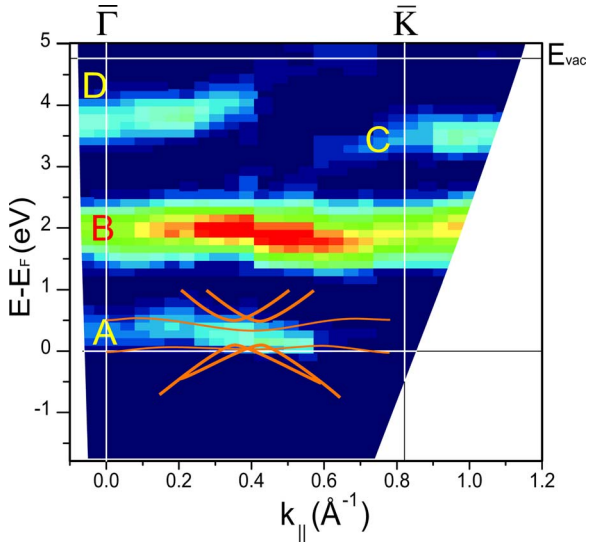

FIG. 7. (Color online) The experimental data are compared with theoretical energy bands calculated by Sánchez-Portal *et al.* (Ref. 18) that include the spin-orbit interaction.

inverse photoemission because the total energy resolution (electrons and photons) is $\Delta E \approx 0.42$ eV (with momentum resolution $\Delta k_{\parallel} \approx 0.1$ Å^{-1}). Despite the fact that the two bands merge into one single feature, the good agreement between the location of the Fermi level crossing obtained from both photoemission and inverse photoemission has the obvious explanation that they are the same feature.

The solid lines in Fig. 6 (S1 and S2) were obtained by fitting parabolas to the experimental energy bands obtained from photoemission.[13] Clearly, our results indicate that the velocity of the S1 and S2 bands decreases above the Fermi level. The parabolic approximation appears to provide a good description of the band only below the Fermi level.

The clean Si(557) surface also has a state located $\approx$0.5 eV above the Fermi level at $\bar{\Gamma}$. This feature is more intense than the corresponding state on Si(557)-Au. Furthermore, it does not appear to cross the Fermi level. Given the state's position and its relatively narrow bandwidth, we identify it as the Si(111)-(7×7) U_1 adatom state.[34] It is not surprising to observe U_1 in these spectra, given that there are regions of 7×7 reconstruction on the Si(557) terraces.[35] Evidence for the 7×7 reconstruction is also present in LEED images from the same surface. We noted above that upon the addition of gold adatoms to the surface, weight is transferred from A$\rightarrow$B. This has the natural explanation that the band derived from the silicon adatoms is modified by the surface reconstruction and the hybridization of silicon atoms with the embedded gold atoms that lie within the silicon terraces.

Our experimental bands will now be compared with the theoretical energy bands calculated by Sánchez-Portal *et al.*[18] using the experimental data from Fig. 5. To our knowledge, this is the only theoretical band structure that is available that uses the minimum energy geometric structure for this reconstruction, other than a calculation by the same group that did not include the spin-orbit interaction.[21] Following the procedure we described above, the data have been mapped to $(E,k_{\parallel})$ and plotted together with the theoretical bands in Fig. 7. The VASP code[36] was used to perform the calculation and the spin-orbit interaction was explicitly incorporated. It should be clear from the figure that an extensive comparison of the two band structures is not possible because the published theoretical bands extend only to 1.0 eV above the Fermi level whereas the experimental bands extend up to 5.0 eV above the Fermi level. Nevertheless, in the energy range where comparison can be made, the position of the calculated Fermi level crossings at $k_{\parallel} \approx 0.45$ Å^{-1} is in agreement with experiment. The dispersion of the calculated band found at $E_F+0.5$ eV also matches the experimental band structure from $k_{\parallel}=0.0-0.5$ Å^{-1}.

We now compare the results of scanning tunneling spectroscopy with our experimental energy bands. In a recent STM study,[23] the normalized differential conductance dI/dV was measured over the step edge at both 78 and 300 K. The differential conductance, using standard approximations,[37] is proportional to the local density of states (LDOS) of the sample multiplied by a smooth transmission function. Consequently, it is possible to make a connection between the LDOS, measured with STM, and the joint density of states, measured by inverse photoemission. The room temperature

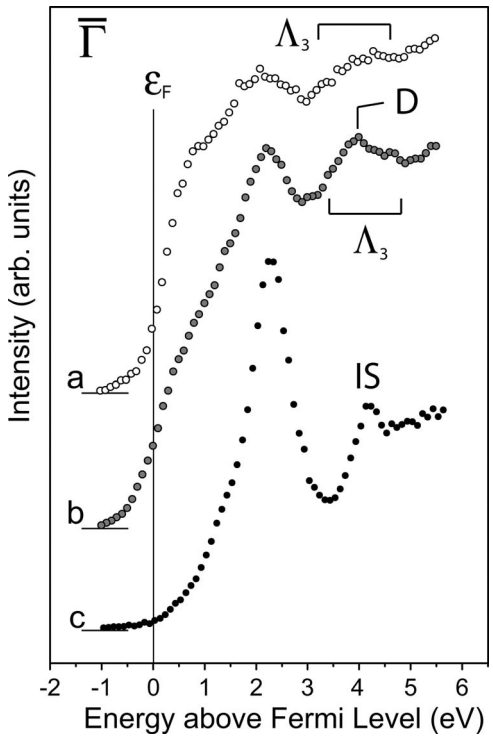

FIG. 8. Inverse photoemission spectra collected from: (a) clean Si(557), and two quasi-1D systems, (b) Si(557)-Au, and (c) Si(111)-In(4×1). The horizontal lines that have been added to each spectrum are baselines representing zero photon intensity.

STS spectra have two features, located just above the Fermi level, that show a splitting similar to the features A and B observed in inverse photoemission near the $\bar{\Gamma}$ point: $\approx$0.9 eV compared with $\approx$1.5 eV in our experiment. The agreement between these two splittings is satisfactory, given the number of simplifying approximations that must be made to allow this comparison.

As mentioned above, there is a different state on the Si(557)-Au system located just below the vacuum level (D in Figs. 5–7). To appreciate this, it is necessary to study the energy distribution curves that, in this energy region, clearly illustrate the differences between the two systems. To aid comparison, we present in Fig. 8 inverse photoemission spectra collected from clean Si(557), Si(557)-Au, and also from Si(111)-In(4×1). The inverse photoemission spectrum from the Si(557) surface (curve a) has a broad feature located $\approx$4.0 eV above the Fermi level. Previous inverse photoemission studies[38,39] performed on the Si(111) surface have assigned this feature to a transition into one of the two lowest conduction bands (Λ_3) located along the ΓL direction in the bulk Brillouin zone of silicon. Furthermore, the dispersion of this state was examined along the $[01\bar{1}]$ direction. It was found that the dispersion of the transition into the bulk Λ_3 band was almost flat about the zone center. Although this transition is not being probed in exactly the same way in our experiment, due to the fact that the terraces in Si(557) are rotated by the offcut angle of 9.5°, this result suggests that the transition into the bulk Λ_3 band should also be present on Si(557) in the same energy range. That is what is observed in Fig. 8(a).

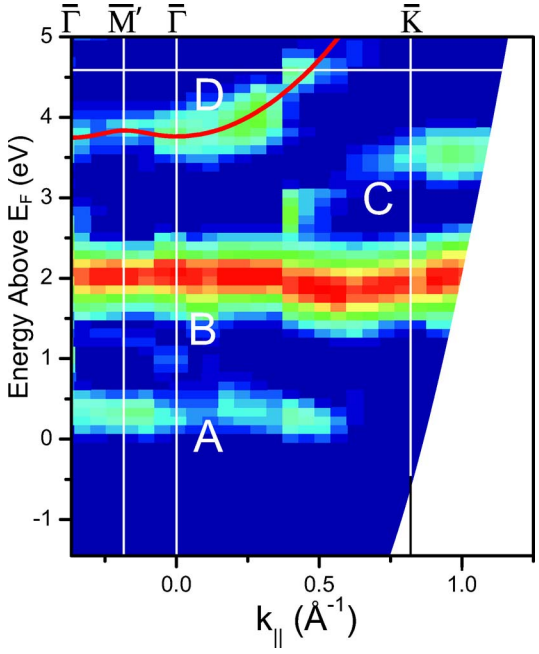

FIG. 9. (Color online) The experimental energy bands along $\overline{\Gamma K}$ and $\overline{\Gamma M'\Gamma}$ are compared. This figure clearly illustrates the quasi-1D nature of state D.

However, on Si(557) (curve b) there is clear evidence for additional weight on top of the Λ_3 bulk transition and this has been labeled, using the convention we adopted earlier, as D. It is not possible to determine either the width or the intensity of this feature with a high degree of precision because it overlaps the transition into the bulk Λ_3 band and the analytical form of the line profile generated by this transition is unknown. However, we can say with confidence that it is broader than the image state resonance that we studied previously on the quasi-1D Si(111)-In(4×1) surface (curve c). The width of the $n=1$ image state in the Si(111)-In(4×1) system is detector-limited, reflecting the instrumental bandpass, and we have used this fact to measure the energy resolution of a number of photon detectors.[26] The width of the corresponding state on Si(557)-Au is much larger, and its intensity is substantially lower than the intensity of the image state resonance on Si(111)-In(4×1). In general, the photon emission from gold-induced reconstructions in this energy range is very weak compared with reconstructions induced by other adsorbates.[27] Fitting a parabolic band to the band around the zone center suggests that the band minimum lies (0.8 ± 0.4) eV below the vacuum level with an effective mass $m^*=(1.0\pm0.1)m_e$, where m_e is the free electron mass. The dispersion of the state, at least around the zone center, is what we would expect for an image state. However, we note that when the energy distribution curves from the Si(557) surface are rendered as an $(E,k_\parallel)$ grid the bulk Λ_3 transition also disperses upwards (Fig. 6). This is in marked contrast to previous studies,[38] mentioned above, that found a completely flat dispersion about the zone center. However, this transition is being probed slightly differently because of the vicinal offcut. Consequently, our results show that state D is superimposed on a bulk transition that also disperses to lower

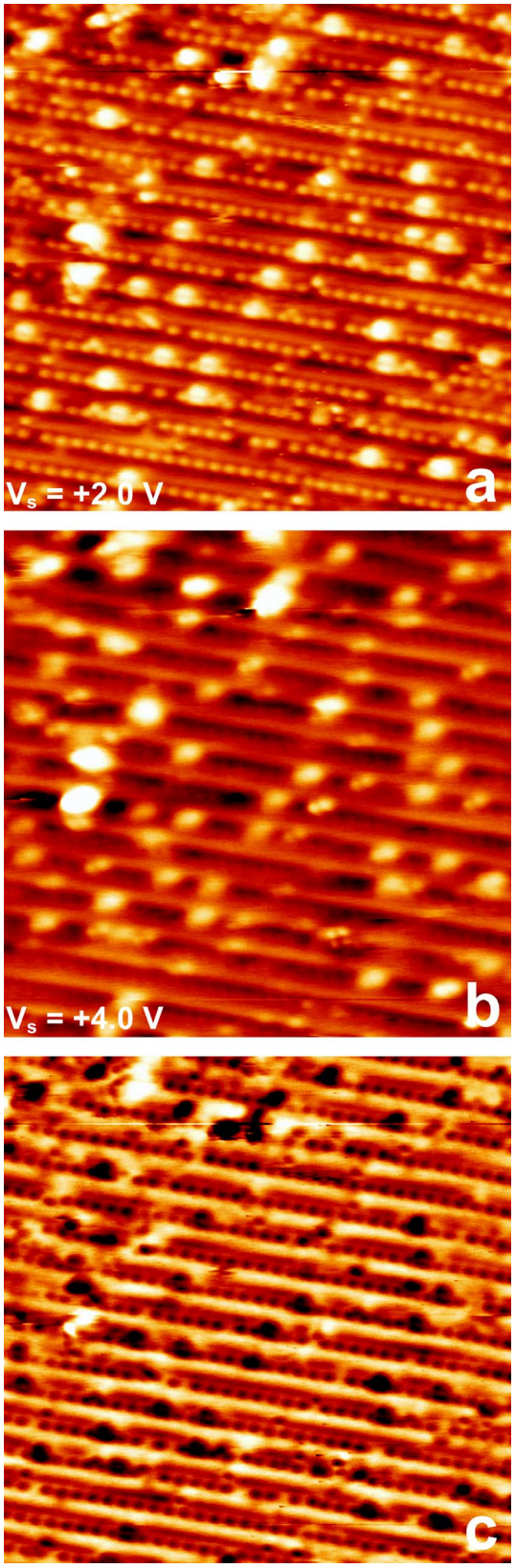

FIG. 10. (Color online) Two STM images of the Si(557)-Au system. The image area is 30 nm$\times$30 nm and in (a) the sample bias was +2.00 V (a higher binding energy than feature D) and in (b) it was +4.00 V (a lower binding energy than feature D). (c) was obtained by subtracting image (a) from image (b) (see the text).

binding energy as the band moves away from the zone center.

In the perpendicular direction (Fig. 9) the dispersion of feature D is quite flat, as we would expect for a quasi-1D band. The other features, A and B, also have a flat dispersion along this direction. The behavior of band D is remarkably similar to the behavior of a one-dimensional step-induced image state that was found previously on vicinal Cu(001) surfaces.[40] We will return to this fact later.

What is the physical origin of feature D? It is unlikely to be a "conventional" image state because there is no band gap in the substrate band structure in this energy range. Consequently, the crystal potential will not Bragg scatter electrons into the surface region. This suggests that at most the state is an image state resonance, similar to the image state resonance found on Al(111).[41,42] This assignment finds support from the large state linewidth because the overlap with the bulk continuum should certainly reduce the lifetime of the state. Consequently, feature D could be an incipient overlayer-induced image state resonance. This similarity between the image states that appear on overlayer systems grown on semiconductors and the image state resonance on Al(111) has been noted before,[43] but it is worth reiterating this in the context of Si(557)-Au. Unfortunately, the physical factors that stabilize image state resonances in ordered overlayer systems on semiconductors, and in particular overlayers with quasi-1D symmetry, are not well-understood. Presumably the surface potential generated by the overlayer system plays an important role in localizing the states within the near surface region, as it does on Al(111). It is unknown what criteria have to be met by the surface potential in these quasi-1D systems to produce an image state resonance with a narrow linewidth. Why, for example, is the image state on Si(111)-In(4×1) so different from the corresponding state on Si(557)-Au?

To determine the spatial location of the image state resonance, two constant-current topographs from the Si(557)-Au system were collected with STM, shown in Figs. 10(a) and 10(b). The biases were chosen to be above and below the band minimum of the image state resonance. STS studies of image states on metal surfaces[44] have shown that the high field between the tip and sample produces a Stark shift in the higher-order members of the Rydberg series. However, the $n=1$ peak, which dominates the inverse photoemission spectrum, was not strongly affected by the electric field. Therefore it is reasonable to assume that the constant-current topographical images collected at $V_s=+4.0$ V contains a contribution from the image state resonance. These biases are very high for STM and we would expect a degradation of the spatial resolution due to the onset of field emission. However, using defects in the topographical images we were able to precisely superimpose the two images and perform a numerical subtraction, as shown in Fig. 10(c). The result of this process yielded stripes that are coincident with the terrace edges. This fact is particularly interesting because recent low temperature STM studies[23] have placed the metallic band at the step edge.

IV. CONCLUSIONS

The unoccupied bands in the quasi-1D Si(557)-Au system have been studied with inverse photoemission. A state was observed to disperse downwards from the zone center at $\bar{\Gamma}$, where it is located (0.4 ± 0.4) eV above the Fermi level, and crosses the Fermi level at $k_{\|}=(0.5\pm0.1)$ Å^{-1}, in excellent agreement with previous photoemission results and *ab initio* calculations.

A second band was observed (0.8 ± 0.4) eV below the vacuum level, close to the binding energy at which an $n=1$ image potential state would be expected. It had a parabolic dispersion along $\overline{\Gamma K}$ and an effective mass $m^*=(1.0\pm0.1)m_e$. Its dispersion in the perpendicular direction $\overline{\Gamma M'\Gamma}$ is fairly flat, indicating that it has quasi-1D symmetry. Although the binding energy and band mass of this state are exactly what we would expect for a quasi-1D image state, the linewidth of the state is extremely large, casting doubts on this interpretation. However, it is possible that the state is an image state resonance that is on the edge of detectability with inverse photoemission. We described it earlier as an *incipient* image state resonance. The rationale for its assignment as an image state resonance is as follows.

Image states are not observed on clean silicon surfaces with inverse photoemission. They are observed only after overlayers have been adsorbed. Therefore, since the adsorption of the overlayer does not change the bulk band structure of the silicon substrate, the surface potential must be changed by the adsorbed layer and the surface potential of the modified surface must be capable of localizing states in the near surface region. What makes this line of argument interesting is the nature of the overlayer systems that support image state resonances; both Si(111)-In(4×1) and Si(557)-Au are quasi-1D systems. In contrast, most studies of image states or image state resonances have been performed on surfaces that possess full two-dimensional symmetry. The effect of reduced dimensionality on electronic structure is a central problem in condensed matter physics and we have here an example of two quasi-1D overlayer systems that have quite different atomic structures, yet both possess image state resonances. However, Si(111)-In(4×1) is, from a structural point of view, a "conventional" quasi-1D system, comprising rows of indium atoms on a flat silicon surface. Si(557)-Au is much more complex, comprising ordered rows of silicon adatoms, metallic step-edge states, and rows of embedded gold atoms. How do these structural features on Si(557)-Au influence the formation of electronic states in the near surface region? What are the physical factors that lead to the localization of the image state on the terrace edges? These are fascinating questions that deserve further theoretical attention.

ACKNOWLEDGMENTS

This research was supported by the Natural Sciences and Engineering Research Council of Canada. The authors benefitted from discussions with G. P. Srivastava and R. H. Miwa.

*Electronic address: mclean@physics.queensu.ca; URL: http://www.physics.queensu.ca/~nanophys

[1] F. D. M. Haldane, J. Phys. C **14**, 2585 (1981).
[2] J. Voit, Phys. Rev. B **47**, 6740 (1993).
[3] E. Bertel, Surf. Sci. **331-333**, 1136 (1995).
[4] A. Dallmeyer, C. Carbone, W. Eberhardt, C. Pampuch, O. Rader, W. Gudat, P. Gambardella, and K. Kern, Phys. Rev. B **61**, R5133 (2000).
[5] F. J. Himpsel, A. Kirakosian, J. N. Crain, J. L. Lin, and D. Y. Petrovykh, Solid State Commun. **117**, 149 (2001).
[6] P. Gambardella, A. Dallmeyer, K. Malti, M. C. Malagoli, W. Eberhardt, K. Kern, and C. Carbone, Nature (London) **416**, 301 (2002).
[7] C. Binns, C. Norris, and S. J. Gurman, J. Phys. C **16**, 417 (1983).
[8] C. Binns and C. Norris, J. Phys.: Condens. Matter **3**, 5425 (1991).
[9] I. G. Hill and A. B. McLean, Phys. Rev. Lett. **82**, 2155 (1999).
[10] P. Segovia, D. Purdie, M. Hengsberger, and Y. Baer, Nature (London) **402**, 504 (1999).
[11] J. N. Crain, J. L. McChesney, F. Zheng, M. C. Gallagher, P. C. Snijders, M. Bissen, C. Gundelach, S. C. Erwin, and F. J. Himpsel, Phys. Rev. B **69**, 125401 (2004).
[12] M. Schöck, C. Sürgers, and H. v. Löhneysen, Thin Solid Films **428**, 11 (2003).
[13] K. N. Altmann, J. N. Crain, A. Kirakosian, J. L. Lin, D. Y. Petrovykh, F. J. Himpsel, and R. Losio, Phys. Rev. B **64**, 035406 (2001).
[14] R. Losio, K. N. Altmann, A. Kirakosian, J. L. Lin, D. Y. Petrovykh, and F. J. Himpsel, Phys. Rev. Lett. **86**, 4632 (2001).
[15] F. J. Himpsel, J. L. McChesney, J. N. Crain, A. Kirakosian, V. Perez-Dieste, N. L. Abbott, Y. Y. Luk, P. F. Nealey, and D. Y. Petrovykh, J. Phys. Chem. B **108**, 14484 (2004).
[16] J. R. Ahn, H. W. Yeom, H. S. Yoon, and I. W. Lyo, Phys. Rev. Lett. **91**, 196403 (2003).
[17] J. N. Crain, A. Kirakosian, K. N. Altmann, C. Bromberger, S. C. Erwin, J. L. McChesney, J. L. Lin, and F. J. Himpsel, Phys. Rev. Lett. **90**, 176805 (2003).
[18] D. Sánchez-Portal, S. Riikonen, and R. M. Martin, Phys. Rev. Lett. **93**, 146803 (2004).
[19] O. Gallus, T. Pillo, M. Hengsberger, P. Segovia, and Y. Baer, Eur. Phys. J. B **20**, 313 (2001).
[20] D. Sánchez-Portal, J. D. Gale, A. García, and R. M. Martin, Phys. Rev. B **65**, 081401(R) (2002).
[21] D. Sánchez-Portal and R. M. Martin, Surf. Sci. **532-535**, 655 (2003).
[22] S. LaShell, B. A. McDougall, and E. Jensen, Phys. Rev. Lett. **77**, 3419 (1996).
[23] H. W. Yeom, J. R. Ahn, H. S. Yoon, I. W. Lyo, H. Jeong, and S. Jeong, Phys. Rev. B **72**, 035323 (2005).
[24] N. G. Stoffel and P. D. Johnson, Nucl. Instrum. Methods Phys. Res. A **234**, 230 (1984).
[25] J. A. Lipton-Duffin, A. G. Mark, and A. B. McLean, Rev. Sci. Instrum. **73**, 3149 (2002).
[26] J. A. Lipton-Duffin, A. G. Mark, G. K. Mullins, G. E. Contant, and A. B. McLean, Rev. Sci. Instrum. **75**, 445 (2004).
[27] I. G. Hill and A. B. McLean, Appl. Surf. Sci. **123/124**, 371 (1998).
[28] A. Lucas, Diploma thesis, University of Stuttgart, 2000.
[29] J. M. MacLeod, A. Moffat, J. A. Miwa, A. G. Mark, G. K. Mullins, R. H. J. Dumont, G. E. Contant, and A. B. McLean, Rev. Sci. Instrum. **74**, 2429 (2003).
[30] K. C. Pandey, Phys. Rev. Lett. **49**, 223 (1982).
[31] S. C. Erwin and H. H. Weitering, Phys. Rev. Lett. **81**, 2296 (1998).
[32] F. J. Himpsel, Adv. Phys. **32**, 1 (1983).
[33] T. Abukawa, M. Sasaki, F. Hisamatsu, T. Goto, T. Kinoshita, A. Kakizaki, and S. Kono, Surf. Sci. **325**, 33 (1995).
[34] J. M. Nicholls and B. Reihl, Phys. Rev. B **36**, 8071 (1987).
[35] A. Kirakosian, R. Bennewitz, J. N. Crain, T. Fauster, J. L. Lin, D. Y. Petrovykh, and F. J. Himpsel, Appl. Phys. Lett. **79**, 1608 (2001).
[36] G. Kresse and J. Furthmüller, Phys. Rev. B **54**, 11169 (1996).
[37] C. J. Chen, *Introduction to Scanning Tunneling Microscopy* (Oxford University Press, New York, 1993).
[38] D. Straub, L. Ley, and F. J. Himpsel, Phys. Rev. Lett. **54**, 142 (1985).
[39] D. Straub and F. J. Himpsel, Phys. Rev. B **33**, 2256 (1986).
[40] J. E. Ortega, F. J. Himpsel, R. Haight, and D. R. Peale, Phys. Rev. B **49**, 13859 (1994).
[41] D. Heskett, K.-H. Frank, E. E. Koch, and H.-J. Freund, Phys. Rev. B **36**, 1276 (1987).
[42] S. Yang, R. A. Bartynski, and D. Vanderbilt, Phys. Rev. B **50**, 12025 (1994).
[43] H. Öfner, S. L. Surnev, Y. Shapira, and F. P. Netzer, Surf. Sci. **307-309**, 315 (1994).
[44] G. Binnig, K. H. Frank, H. Fuchs, N. Garcia, B. Reihl, H. Rohrer, F. Salvan, and A. R. Williams, Phys. Rev. Lett. **55**, 991 (1985).